Frequency Support of Fast-Multi-Energy Storage Systems in Low Rotational Inertia Scenarios

Ersdal, Anne Mai[1]; Acosta Montalvo, Martha Nohemi[2,3]; Gonzalez-Longatt, Francisco[2]; Rueda Torres, Jose Luis[4]; Palensky, Peter[4]

[1]Institutt for automasjon og prosessteknologi - UiT The Arctic University of Norway
[2]Department of Electrical engineering, Information Technology and Cybernetics - University of South-Eastern Norway
[3]Autonomous University of Nuevo León - Autonomous University of Nuevo León
[4]Technische Universiteit Delft - Delft University of Technology

Ersdal, A. M., Gonzalez-Longatt, F., Acosta, M. N., Rueda, J. L., & Palensky, P. (2020, October 26-28). Frequency Support of Fast-Multi-Energy Storage Systems in Low Rotational Inertia Scenarios. In *2020 IEEE PES Innovative Smart Grid Technologies Europe (ISGT-Europe)* (p. 879-883). https://doi.org/10.1109/ISGT-Europe47291.2020.9248843

Publisher's version: DOI: 10.1109/ISGT-Europe47291.2020.9248843

Frequency Support of Fast-Multi-Energy Storage Systems in Low Rotational Inertia Scenarios

Anne Mai Ersdal
Department of Automation and Process Engineering
The Arctic University of Norway
Tromso, Norway
anne.mai.ersdal@uit.no

Martha N. Acosta
School of Mechanical and Electrical Engineering
Universidad Autónoma de Nuevo León
Nuevo León, México
martha.acostamnt@uanl.edu.mx

F. Gonzalez-Longatt
Martha N. Acosta
Department of Electrical engineering, Information Technology and Cybernetics
University of South-Eastern Norway
Porsgrunn, Norway
fglongatt@fglongatt.org

J.L. Rueda
Department of Electrical Sustainable Energy
Delft University of Technology (TU Delft)
Delft, Netherlands
J.L.RuedaTorres@tudelft.nl

P. Palensky
Department of Electrical Sustainable Energy
Delft University of Technology (TU Delft)
Delft, Netherlands

***Abstract*— Modern power systems are increasing the connection of power electronic converters (PECs), and new inertia-less technologies displace the synchronous generation units. Therefore, the total rotational system inertia is reduced, creating new problems related to the system frequency control and stability. Several mechanisms to enable the PECs with frequency sensible control loops have been proposed in the scientific literature. This paper considers the use of Fast-Acting Power Injections (FAPI), where the frequency-sensible control uses a frequency-active power (*f-P*) based on proportional and derivative control. The FAPI is obtained from PECs installed in a Fast-Multi-Energy Storage System (F-MESS), it consists of a flywheel storage system and supercapacitor storage system. The objective is to assess the frequency support provided by an F-MESS considering low rotational inertia scenarios. One additional contribution is a full detailed model using a set of differential-algebraic equation (DAE) in order to ensure an appropriate representation of all devices at the time that ensure scalability of the model in order to include new PEC-based technologies. Simulation results demonstrate the positive effect of the use of FAPI controllers in F-MESS to provide frequency support in low inertia scenarios.**

Keywords*— *Frequency Control, Low inertia, Multi-energy storage system, Nordic Power System.

I. INTRODUCTION

Modern power systems are evolving quite fast, and the new technologies for power generation and energy storage are helping to cope with the environmental need to reduce CO_2 emission and stabilising a low carbon society [1]. On the other side of the power system, demand side, technical development, especially those related to the use of ICT, are making the demand more controllable, flexible and price sensible [2], [3]. Independently of the side (generation or demand), one key element in the modern power system evolution is the massive use and deployment of power electronics converters (PECs) [4].

The design and the control of PECs for power systems applications have positively evolved in recent times, making the huge advances in many fields, including the improvement on the power quality footprints [5]. However, the integration of technologies based on PECs creates some problems, one of them is related with the progressive replacement of synchronous machines based generation unit by PECs-based technologies, as a consequence, there is an inherent reduction in the total system rotational inertia [4]. As the total physical rotational inertia provided by synchronous generators is reducing, the dynamic related to the frequency is becoming volatile, and negatively affecting the capacity of the power system to recover to system frequency disturbances [6].

The low value of total rotational inertia increases the likelihood of very fast electromechanical dynamics in the power systems arising the possibility of instability [7]. Consequently, the ability to overcome system frequency disturbances decrease based on a decreased inertial response with overwhelming consequences for system frequency security and reliability [8]. Several mechanisms to enable the PECs with frequency sensible control loops have been proposed, the main purpose of all of them is to produce an active power reference signal that is fed into the PECs when the frequency change of some limits or specifications. The set of controllers that follow that frequency-active power (*f-P*) control rule are defined in this paper as *Fast-Acting Power Injections* (FAPI) [9].

The *fast-active power* (FAP) controller is characterised by an extremely fast response (within 1 sec), with a very short time-delay (related to measurement rather than activation). The FAP controller is frequency sensitive controller, where proportional (*K-f*) and derivative (df/dt) control actions are considered together to mimic the inertia response [10]. As the inertia is reduced in the power system, the use of FAP controller with very fast energy systems looks like a promising solution to enhance the system frequency response (SFR). Several recent scientific papers have been dedicated to the use of an electrical energy storage system to provide FAPI and results of [1] demonstrate the suitability of the use of multi-energy storage system MESS to provide FAPI.

This research paper presents an assessment of the frequency support provided by *fast-Multi-Energy Storage Systems* (F-MESS) in considering decreased inertia scenarios. F-MESS is a combination of two very fast electrical energy storage system: supercapacitor and flywheel. The frequency-sensible controller used is based in a FAP controller considering the combination of proportional (K_1-*f*) and proportional-derivative (K_2df/dt) control actions. Furthermore, the measurements of frequency deviation (Δf) are taken as reliable input for the FAP controller. Discussion

about system modelling is presented in Section II. Then, the frequency response model is used to assess the frequency support provided by the F-MESS, considering low inertia scenarios. Numerical results of time-domain simulations are used to assess the frequency support provided by the F-MESS. The assessment is based on main indicators of the SFR, and the FAPI, simulations results indicated the use of F-MESS can deliver very fast active power during the system frequency response and support the frequency, increasing the minimum frequency and enhancing the SFR. Beyond that, this paper contributes to the scientific community by providing a full detailed model of the F-MESS.

II. System Frequency Response Modelling

A. Power System Modelling including F-MESS

The SFR model has been enhanced by including the models of the F-MESS. Consider a large system in which most of the generating units are reheat steam turbine units. The idea of the SFR model is to reduce the power system to one described by a minimum number of equations that will compute only the average frequency behaviour. Typically the SFR model is represented in the form of a combination of block diagrams and transfer function as presented in [11]. However, it is required the full detailed model using a set of differential-algebraic equation (DAE) to ensure an appropriate representation of all devices at the time that ensure scalability of the model to include new PEC-based technologies. In this paper, the authors made an effort to include a frequency response model of F-MESS.

The power system is assumed to have three-control areas, $N = 3$ (see Fig. 1). However, the reader might find it extremely easy to generalize and extend the modelling process to a generic number of control-areas. Three main elements constitute each control area: (i) a turbine-governor system together with a rotating mass and load, (ii) a Fast-Multi-Energy Storage System (F-MESS) and (iii) inter-tie connecting the control area to the other areas inside the power system. Full detail of the dynamic models used in each element is presented in the next subsections.

B. Turbine-governor, rotating mass and load

The i-th control area in an N-control area power system is modelled using an equivalent model that lumps the effects of system loads and generators, considering single inertia constant (H_i) and damping (D_i) coefficient. The single inertia constant is the sum of the inertia constant of all the generating units inside the i-th control area. The following first-order differential equation defines the dynamic of the frequency deviation Δf from the steady-state point (f_0, rated frequency) in the i-th control area:

$$\Delta \dot{f}_i = \frac{1}{2H_i}\left(\Delta P_{mi} + \Delta P_{MESSi} - \Delta P_{Li} - \Delta P_{tiei}\right) \tag{1}$$

where ΔP_{mi} is the change on the produced mechanical power, ΔP_{MESSi} the change on power delivered by the F-MESS, ΔP_{Li} the change on load power, ΔP_{tiei} the deviation of tie-line power leaving the i-th control area, and $i = 1,\ldots,N$. The dynamic related to the reheat steam generator unit is described by:

$$\Delta \dot{P}_{mi} = \frac{1}{T_{ti}}\left(\Delta P_{gi} + \Delta P_{mi}\right) \tag{2}$$

$$\Delta \dot{P}_{gi} = \frac{1}{T_{gi}}\left(\Delta P_{ci} - \frac{1}{R_i}\Delta f_i - \Delta P_{gi}\right) \tag{3}$$

where ΔP_{gi} is the change in the output from the governor to the turbine, ΔP_{ci} is the change in the output from the secondary control loop altering the production set point to the governor, T_{ti} and T_{gi} are time constants of the turbine and governor, and R_i the droop. In this research paper, the dynamic of the tie-line power control, together with the algebraic model of the simplified transmission system is included as [11]:

$$\Delta \dot{P}_{ci} = K_{si}\left(\Delta P_{tiei} + \beta_i \Delta f_i\right) \tag{4}$$

$$\Delta \dot{P}_{tiei} = 2\pi \mathbf{M}\Delta\mathbf{f} \tag{5}$$

where K_{si} is the secondary control gain, β_i the bias factor, $\mathbf{M}$ the synchronising coefficient matrix, and $\Delta\mathbf{f} = [\Delta f_1\ \Delta f_2\ \Delta f_3]^T$.

C. Fast-Multi-energy storage system (F-MESS)

Frequency control in low inertia systems requires a high-speed injection of frequency dependant active power. Therefore, new technologies are increasing participation in high-speed frequency services, flywheel, supercapacitors, and some batteries technologies can provide full power in less than second scales. The main interest is the frequency control at low inertia system; therefore, two energy storage technologies are considered: (i) Flywheel, and (ii) supercapacitor.

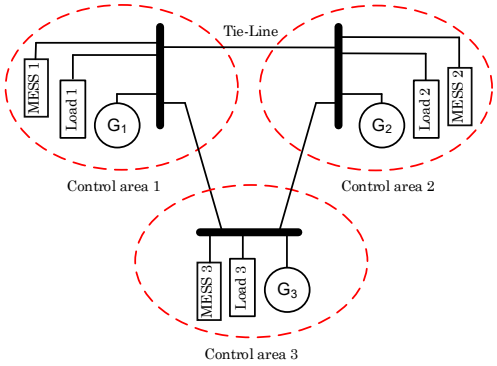

Fig. 1. Test system: three-control area power system, including F-MESS

1) Flywheel

The i-th area consists of several flywheels, and the dynamic behaviour of each flywheel j is represented by a set of first-order differential equations defining the electromechanical dynamics of the flywheel [1]:

$$\begin{aligned}
\dot{\omega}_{ij} &= -\frac{1}{J_{ij}}\,sat\left(\frac{z_{FW1ij}}{\omega_{ij}}\right) \\
\dot{z}_{FW1ij} &= -\frac{1}{T_{dij}}\left(z_{FW2ij} - z_{FW1ij}\right) \\
\dot{z}_{FW2ij} &= 8\left(\frac{\Delta P_{FWsp,i}}{K_{FWunits,i}} - sat\left(\frac{z_{FW1ij}}{\omega_{ij}}\right)\omega_{ij}\right)
\end{aligned} \tag{6}$$

where ω_{ij} [rad/s] is the angular velocity, z_{FW1ij} [p.u.] and z_{FW2ij} [p.u.] internal states associated with the delay introduced by the power converter and the internal controller, respectively. J_{ij} [kg·m^2] is the moment of inertia of the flywheel, T_{di} [s] a time delay, $K_{FWunits,i}$ [-] the number of flywheels in the i-th area, $P_{FWsp,i}$ [p.u.] the set point for total power delivery from all flywheels in area i, and $j = 1,..,K_{FWunits,i}$. From this, the total

delivered power from the flywheels in each area P_{FWi} [p.u.] and state of charge (SOC) [%] can be calculated as follows:

$$\Delta P_{FWi} = \sum_{j=1}^{K_{FWunits,i}} sat\left(\frac{z_{FW1ij}}{\omega_{ij}}\right)\omega_{ij}$$
$$SOC_{FW} = \frac{1}{K_{FWunits,i}} \sum_{j=1}^{K_{FWunits,i}} \frac{\omega_{ij}^{\ 2}}{\omega_{\max,ij}^2} \quad (7)$$

where $\omega_{\max,ij}$ is the maximum angular velocity of the flywheel.

The contribution from the flywheels is controlled based on the frequency deviation in each area using a proportional controller with proportional gain $K_{FWp,i}$:

$$\Delta P_{FWsp,i} = -K_{FWp,i}\Delta f_i \quad (8)$$

and the contribution from the flywheels is included in the N-control area model by adding the following to ΔP_{MESSi}:

$$\Delta P_{MESSi} = \frac{\Delta P_{FWi} P_{baseFW,i}}{S_{base}} \quad (9)$$

where $P_{baseFW,i}$ [W] and S_{base} [W] is the active power base for the flywheels and the N-control area model, respectively.

2) Supercapacitor

The i-th area consists of several supercapacitors. The dynamic behaviour of the j-th supercapacitor is represented by the differential equations [1], [12]:

$$\dot{z}_{SCij} = -\frac{1}{T_{dij}}\left(\frac{\Delta P_{SCsp,i}}{K_{SCunits,i}} - z_{SCij}\right)$$
$$\dot{Q}_{ij} = -\frac{z_{SCij} P_{baseSC,i}}{V_{SCij}} \quad (10)$$

where Q_{ij} [C] is the electric charge, z_{SCij} [p.u.] an internal state representing the power converter delay, $\Delta P_{SCsp,i}$ [p.u.] the set point for total power delivery from all supercapacitors in area i, V_{SCi} [V] the voltage over the supercapacitor, T_{dij} [s] a time constant, $K_{SCunits,i}$ [-] the number of supercapacitors in area i, $P_{baseSC,i}$ [W] the active power base of the supercapacitors and $j = 1,..,K_{SCunits,i}$. The expression for V_{SCij} is as follows.

$$V_{Tij} = \frac{N_{sij} d_{ij} Q_{ij}}{N_{pij} N_{eij} \varepsilon_{ij} A_{ij}} + \frac{2N_{eij} N_{sij} R T_{ij}}{N_{pij} F} a\sinh\left(\frac{Q_{ij}}{N_{eij}^2 A_{ij}\sqrt{8RT_{ij}\varepsilon_{ij} c_{ij}}}\right)$$
$$V_{SCij} = \frac{V_{Tij} + \sqrt{V_{Tij}^2 - 4R_{SCij}\frac{z_{SCij} P_{SCbase,i}}{K_{SCunit,i}}}}{2} \quad (11)$$

where V_{Tij} [V] is the internal voltage, N_{sij} [-] and N_{pij} [-] are the number of series and parallel supercapacitors, respectively. d_{ij} [m] the molecular radius, N_{eij} [-] the number of layers of electrodes, ε_{ij} [F/m] the absolute permittivity of the material, A_{ij} [m^2] the interfacial area between electrodes and electrolyte, R [J/mol·K] the ideal gas constant, T_{ij} [K] the operating temperature, F [sA/mol] the Faraday constant, c_{ij} [mol/m^3] the molar concentration and R_{SCij} [Ω] the internal resistance. The SOC [%] of the supercapacitor is calculated as:

$$SOC_{SC} = \frac{100}{K_{SCunits,i}} \sum_{j=1}^{K_{SCunits,i}} \frac{Q_{ij}}{Q_{rated,ij}} \quad (12)$$

and the total delivered power from the supercapacitors in each area ΔP_{SCi} [p.u.] can be calculated as follows:

$$i_{SCij} = \frac{z_{SCij} P_{baseSC,i}}{V_{SCij}}$$
$$\Delta P_{SCi} = \frac{\sum_{j=1}^{K_{SCunits,i}} i_{SCij} V_{SCij}}{P_{baseSC,i}} \quad (13)$$

where i_{SCij} [A] is the current in each supercapacitor.

The contribution from the supercapacitors is controlled based on the frequency deviation in each area using a proportional controller with proportional gain $K_{SCp,i}$:

$$\Delta P_{SCsp,i} = -K_{SCp,i}\Delta f_i \quad (14)$$

and the contribution from the supercapacitors is included in the N-control area model by expanding (9) to

$$\Delta P_{MESSi} = \frac{\Delta P_{FWi} P_{baseFW,i}}{S_{base}} + \frac{\Delta P_{SCi} P_{baseSC,i}}{S_{base}} \quad (15)$$

III. System Frequency Response Assessment

The objective of this paper is to assess the frequency support provided by an F-MESS considering low rotational inertia scenarios.

A. Test system description

The full detailed DAE model presented in the previous section has been implemented using MATLAB® R2019b. All equations are implemented by the authors and solved using the solver ode15s(). The test system consists of three-control areas, $N = 3$ (see in Fig. 1), each control areas is equipped with an F-MESS: Flywheel energy storage system (FESS) and supercapacitor energy storage systems (SESS) (Numerical details of the model parameters from [1], [11].) The system frequency response is evaluated using two main variables: frequency deviation from the steady-state point (Δf) and the change on power delivered by the F-MESS (ΔP_{MESS}).

A sudden step increases in the load demand in Area 1 and Area 3*:* $\Delta P_{L1} = \Delta P_{L3} = 0.02$ p.u. applied at $t = 1.0$ sec is used as a system frequency disturbance. For all cases, three indicators of the SFR are observed: (i) maximum frequency deviations (Δf_{max}), (ii) minimum frequency (f_{min}), and (iii)minimum time (t_{min}). Regarding the active power contribution of the F-MESS, the main indicator to consider is the maximum active power deviation of the combination of SESS and FESS ($\Delta P^{\max}_{MESS}$).

B. Definition of scenarios

The low inertia conditions are evaluated considering three simulation scenarios: *Scenario I* present frequency deviations (Δf) and the active power contribution of the F-MESS (ΔP_{MESS}) considering the nominal amount of inertia in each area, i.e., $H_i = H_{0i}\ \forall\ i = 1, 2, \ldots, N = 3$ (where H_{0i} is the nominal inertia of each control area). *Scenario II* evaluate Δf and ΔP_{MESS} when the inertia decreases 25% in each area, i.e., $H_i = 0.75H_{0i}$. Finally, *Scenario III* consider a reduction in the inertia of 50%, i.e., $H_i = 0.5H_{0i}$. Furthermore, each scenario evaluates two cases: *Case I* refers to the natural Δf response of the system without any F-MESS and *Case II* study the Δf response of the system considering F-MESS.

C. Numerical Results

Scenario I: In this scenario, the system inertia in each area does not change. Therefore, $H_1 = H_{01} = 0.0833$sec, $H_2 =$

H_{02}=1.008sec and H_3=H_{03}=0.0624sec for Area 1, Area 2 and Area 3, respectively. For this scenario, *Case I* present the frequency deviation after the system frequency disturbance when it is not considered the active power supply by F-MESS, and it is shown in Fig. 2. In this figure, Δf_{max} is generated in Area 2 with a value of $\Delta f_{max,2}$= −0.062Hz and f_{min}=49.938 Hz. Moreover, in *Case II*, Δf and ΔP_{MESS} are presented in Fig. 3. The contribution of the F-MESS causes an improvement in the minimum frequency from f_{min}=49.938Hz in *Case I* to f_{min}=49.942Hz.

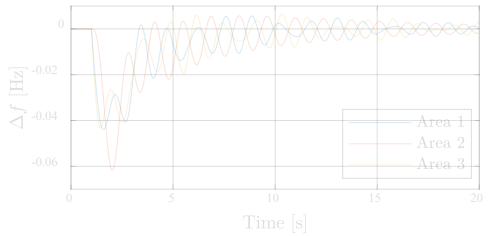

Fig. 2. *Scenario I* ($H_i = H_{0i}$), *Case I:* frequency deviation (Δf).

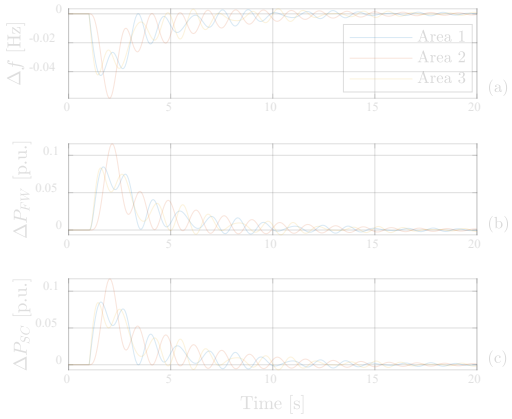

Fig. 3. *Scenario I* ($H_i = H_{0i}$), *Case II*: (a) Frequency deviation (Δf) and power delivered by (b) flywheel (ΔP_{FW}) and (c) supercapacitor (ΔP_{SC}).

Table I present the SFR indicators and $\Delta P^{max}{}_{MESS}$ for *Case I* and *Case II.* It can be observed that $\Delta P^{max}{}_{MESS}$ delivered by FESS and SESS is 0.1696 p.u., 0.2323 p.u. and 0.1676 p.u. in Area 1, Area 2 and Area 3, respectively. Therefore, f_{min} in *Case II* decrease 3.1%, 5.3% and 2.4% in Area 1, Area 2 and Area 3, respectively, concerning *Case I*.

TABLE I. SFR INDICATORS AND THE MAXIMUM ACTIVE POWER RELEASED BY F-MESS USING THE ORIGINAL INERTIA, SCENARIO I

Indicator	Area 1		Area 2		Area 3	
	Case I	*Case II*	*Case I*	*Case II*	*Case I*	*Case II*
Δf_{min} (Hz)	−0.044	−0.043	−0.062	−0.058	−0.043	−0.042
f_{min} (Hz)	49.956	49.957	49.938	49.942	49.957	49.958
t_{min} (s)	1.585	1.559	2.006	2.027	1.427	1.419
ΔP^{max}_{MESS} (p.u.)	—	0.1696	—	0.2323	—	0.1676

Scenario II: In this scenario, the system inertia decreases 25% from its nominal values in each area, i.e., $H_1 = 0.75H_{01} = 0.0625$sec, $H_2 = 0.75H_{02} = 0.0756$sec and $H_3 = 0.75H_{03} = 0.0468$ sec. Fig. 4 shows Δf when the action of F-MESS is not contemplated (*Case I)* and it is observed that Area 2 has the maximum frequency deviation as $\Delta f_{max,2}$= −0.070 Hz and f_{min} = 49.930 Hz. Moreover, the effect of reducing the inertia is reflected in the minimum frequency since it falls 0.008 Hz and t_{min} diminish 0.147 sec. Meanwhile, when the action of F-MESS are considered (*Case II*), Fig. 5 shows (a) Δf, (b) ΔP delivered by FESS and (c) ΔP delivered by SESS. In this case, the minimum frequency and minimum time occurred in Area 2, and its values are f_{min}=49.934Hz and t_{min}=1.836sec. Moreover, the maximum active power was ΔP_{FW}=0.1294p.u. and ΔP_{SC}=0.1318p.u.

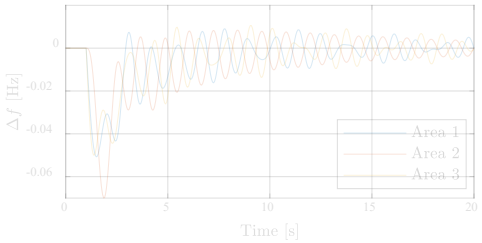

Fig. 4. *Scenario II* ($H_i = 0.75H_{0i}$), *Case I:* frequency deviation (Δf).

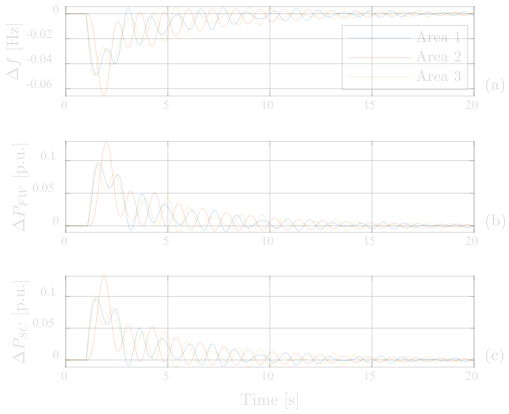

Fig. 5. *Scenario II* ($H_i = 0.75H_{0i}$), *Case II*: (a) Frequency deviation (Δf) and power delivered by (b) flywheel (ΔP_{FW}) and (c) supercapacitor (ΔP_{SC}).

The SFR indicators and $\Delta P^{max}{}_{MESS}$, for *Case I* and *Case II*, are described in Table II. In this scenario, taking *Case I* as a reference: (i) the minimum frequency in *Case II* changes 3.2% in Area 1, 5.9% in Area 2 and 2.3% in Area 3. Furthermore, t_{min} decreases due to the reduction of inertia and the amount of ΔP_{MESS} grow.

TABLE II. SFR INDICATORS AND THE MAXIMUM ACTIVE POWER RELEASED BY F-MESS USING DECREASING THE INERTIA 25%, SCENARIO II

Indicator	Area 1		Area 2		Area 3	
	Case I	*Case II*	*Case I*	*Case II*	*Case I*	*Case II*
Δf_{min} (Hz)	−0.051	−0.049	−0.070	−0.050	−0.043	−0.049
f_{min} (Hz)	49.949	49.951	49.930	49.934	49.950	49.951
t_{min} (s)	1.497	1.490	1.859	1.836	1.407	1.369
ΔP^{max}_{MESS} (p.u.)	—	0.1949	—	0.2613	—	0.1920

Scenario III: This scenario presents the dynamic results of reducing the inertia to 50% of its original value in each control area. The resulting inertia is $H_1 = 0.5H_{01} = 0.0417$sec, H_2=0.5 H_{02} = 0.0504sec and H_3 = 0.5H_{03} = 0.0312sec. From this scenario, in *Case I,* f_{min}=49.916Hz and t_{min}=1.721sec occur in Area 2 (see Fig. 6). Due to the low inertia, these two values decreasing 0.022 Hz and 0.285sec, respectively, regarding *Scenario I*, *Case I.* Furthermore, in *Case II,* the maximum power supplied by F-MESS are ΔP_{FW} =0.1526p.u. and

ΔP_{SC}=0.1577p.u. in Area 2. The minimum frequency and minimum time are f_{min} = 49.921Hz and t_{min} =1.702sec (see Fig. 7).

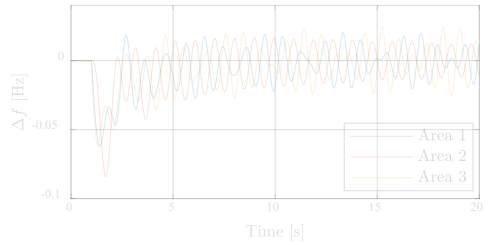

Fig. 6. *Scenario III ($H_i = 0.5H_{0i}$), Case I:* frequency deviation (Δf).

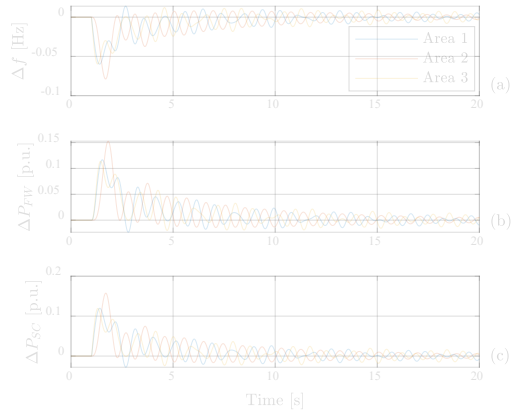

Fig. 7. *Scenario III ($H_i = 0.5H_{0i}$), Case II*: (a) Frequency deviation (Δf) and power delivered by (b) flywheel (ΔP_{FW}) and (c) supercapacitor (ΔP_{SC}).

Table III presents the SFR indicators and $\Delta P^{max}{}_{MESS}$ for *Case I* and *Case II.* In *Case II, f_{min}* decrease 3.6%, 6.2% and 2.69% in Area 1, Area 2 and Area 3, respectively, concerning *Case I*. Therefore, $\Delta P^{max}{}_{MESS}$ required to improve the minimum frequency are 0.2367p.u., 0.3103p.u. and 0.2329 p.u. in Area 1, Area 2 and Area 3, respectively.

TABLE III. SFR INDICATORS AND THE MAXIMUM ACTIVE POWER RELEASED BY F-MESS USING DECREASING THE INERTIA 50%, SCENARIO III

Indicator	Area 1		Area 2		Area 3	
	Case I	*Case II*	*Case I*	*Case II*	*Case I*	*Case II*
Δf_{min} (Hz)	−0.062	−0.060	−0.084	−0.079	−0.061	−0.060
f_{min} (Hz)	49.938	49.940	49.916	49.921	49.939	49.921
t_{min} (s)	1.402	1.382	1.721	1.702	1.326	1.314
ΔP^{max}_{MESS} (p.u.)	—	0.2367	—	0.3103	—	0.2329

The active power delivered by the F-MESS (ΔP_{MESS}) in *Scenario II* increases 14.92%, 12.44% and 14.57% in Area 1, Area 2 and Area 3, respectively concerning *Scenario I*. Meanwhile, in *Scenario III* ΔP_{MESS} rises 39.55% in Area 1, 33.58% in Area 2 and 38.95% in Area 3 relating to *Scenario I*. Therefore, the total amount of ΔP_{MESS} injected in the power system for a given disturbance depends on the quantity of inertia in the power system.

IV. CONCLUSIONS

The proposed DAE model, including F-MESS, has been evaluated considering low inertia operational scenarios. From the simulation results, it has been found that the inclusion of energy storage technologies (F-MESS: FESS and SESS) in the power system improves the frequency response indicators. Low values of inertia produce faster and more profound changes in the frequency and therefore, the time at which the frequency reaches its maximum deviation decrease (*Case I*). However, the inclusion of F-MESS (*Case II*) produces a reduction of the maximum frequency deviation, and as a consequence, the minimum frequency value grows. The active power delivered by F-MESS try to substitute the rotational energy lost when the inertia decreases. Therefore, having the same disturbance, the amount of active power delivered by the F-MESS increase as the inertia decreases.

ACKNOWLEDGMENT

Ms Martha N. Acosta wants to acknowledge the financial support given by CONACYT (México) and the support of Universidad Autónoma de Nuevo León, Mexico, and University of South-Eastern Norway, Norway.

REFERENCES

[1] F. Sanchez, J. Cayenne, F. Gonzalez-Longatt, and J. L. Rueda, "Controller to Enable the Enhanced Frequency Response Services from a Multi-Electrical Energy Storage System," *IET Gener. Transm. Distrib.*, Nov. 2018.

[2] F. A. Alshehri *et al.*, "Generic Model of PEM Fuel Cells and Performance Analysis in Frequency Containment Period in Systems with Decreased Inertia," in *IEEE International Symposium on Industrial Electronics*, 2019, vol. 2019-June, pp. 1810–1815.

[3] R. Puangsukra, J. G. Singh, W. Ongsakul, and F. M. Gonzalez-Longatt, "Multi-Objective Optimization for Enhancing System Coordination Restoration by Placement of Fault Current Limiters on an Active Distribution System with System Reliability Considerations," in *Proceedings of the Conference on the Industrial and Commercial Use of Energy, ICUE*, 2019, vol. 2018-October.

[4] A. J. S. J. Veronica, N. S. Kumar, and F. Gonzalez-Longatt, "Robust PI controller design for frequency stabilisation in a hybrid microgrid system considering parameter uncertainties and communication time delay," *IET Gener. Transm. Distrib.*, vol. 13, no. 14, pp. 3048–3056, Jul. 2019.

[5] H. Chamorro, F. Gonzalez, K. Rouzbehi, R. Sevilla, H. Chavez, and V. Sood, "Innovative Primary Frequency Control in Low-Inertia Power Systems Based on Wide-Area RoCoF Sharing," *IET Energy Syst. Integr.*, Feb. 2020.

[6] A. G. Tobon, H. R. Chamorro, F. Gonzalez-Longatt, and V. K. Sood, "Reliability Assessment in Transmission Considering Intermittent Energy Resources," in *2019 IEEE 10th Latin American Symposium on Circuits and Systems, LASCAS 2019 - Proceedings*, 2019, pp. 193–196.

[7] A. Ulbig, T. S. Borsche, and G. Andersson, "Impact of low rotational inertia on power system stability and operation," in *IFAC Proceedings Volumes (IFAC-PapersOnline)*, 2014, vol. 19, no. 3, pp. 7290–7297.

[8] H. R. Chamorro, I. Riaño, R. Gerndt, I. Zelinka, F. Gonzalez-Longatt, and V. K. Sood, "Synthetic inertia control based on fuzzy adaptive differential evolution," *Int. J. Electr. Power Energy Syst.*, vol. 105, pp. 803–813, Feb. 2019.

[9] F. Gonzalez-Longatt, J. Rueda, and E. Vázquez Martínez, "Effect of Fast Acting Power Controller of Battery Energy Storage Systems in the Under-frequency Load Shedding Scheme," in *International Conference on Innovative Smart Grid Technologies (ISGT Asia 2018)*, 2018.

[10] F. Gonzalez-Longatt, E. Chikuni, and E. Rashayi, "Effects of the Synthetic Inertia from wind power on the total system inertia after a frequency disturbance," in *Proceedings of the IEEE International Conference on Industrial Technology*, 2013, pp. 826–832.

[11] H. Bevrani, *Robust Power System Frequency Control*, Second Edi. Cham: Springer International Publishing, 2014.

[12] H. Miniguano, A. Barrado, C. Fernández, P. Zumel, and A. Lázaro, "A general parameter identification procedure used for the comparative study of supercapacitors models," *Energies*, vol. 12, no. 9, May 2019.